Available online at www.sciencedirect.com
ScienceDirect
Comput. Methods Appl. Mech. Engrg. 310 (2016) 694–710
Computer methods in applied mechanics and engineering
www.elsevier.com/locate/cma

Isogeometric block FETI-DP preconditioners for the Stokes and mixed linear elasticity systems

L.F. Pavarino, S. Scacchi*

Dipartimento di Matematica, Università degli Studi di Milano, Via Saldini 50, 20133 Milano, Italy

Received 8 May 2016; received in revised form 8 July 2016; accepted 12 July 2016
Available online 28 July 2016

Highlights

- We construct a block FETI-DP preconditioner for isogeometric analysis of Stokes and mixed linear elasticity systems.
- We prove that the resulting algorithm is scalable in the number of subdomains and has a quasi-optimal convergence rate bound.
- Extensive two-dimensional numerical experiments validate the theoretical estimates and show the robustness of the method with respect to domain deformation, material incompressibility and presence of elastic coefficient discontinuities across subdomain interfaces.

Abstract

The aim of this work is to construct and analyze a FETI-DP type domain decomposition preconditioner for isogeometric discretizations of the Stokes and mixed linear elasticity systems. This method extends to the isogeometric analysis context the preconditioner previously proposed by Tu and Li (2015) for finite element discretizations of the Stokes system. The resulting isogeometric FETI-DP algorithm is proven to be scalable in the number of subdomains and has a quasi-optimal convergence rate bound which is polylogarithmic in the ratio of subdomain and element sizes. Extensive two-dimensional numerical experiments validate the theory, investigate the behavior of the preconditioner with respect to both the spline polynomial degree and regularity, and show its robustness with respect to domain deformation, material incompressibility and presence of elastic coefficient discontinuities across subdomain interfaces.

Keywords: Isogeometric analysis; Block FETI-DP preconditioners; Stokes and mixed linear elasticity systems; Domain decomposition methods

1. Introduction

While Isogeometric Analysis (IGA) has been introduced more than a decade ago by Hughes et al. [1], see also [2], as an innovative discretization technique for partial differential equations (PDEs), the study of scalable and efficient iterative solvers for IGA discretizations has started only recently, see [3–11] and has focused on elliptic problems. The

* Corresponding author.
E-mail addresses: luca.pavarino@unipv.it (L.F. Pavarino), simone.scacchi@unipv.it (S. Scacchi).

http://dx.doi.org/10.1016/j.cma.2016.07.012
0045-7825/

main challenges that IGA solvers have to face are the extreme ill-conditioning of IGA discretizations with increasing polynomial degrees and the nature of spline and NURBS basis functions, which are not nodal, have large support and lead to wide (fat) interface problems between subdomains. The extension of IGA solvers to saddle point problems, such as the Stokes and mixed linear elasticity systems, has to face the additional challenge arising from the continuous pressures employed in stable IGA mixed discretizations, see [12].

The goal of this work is to address such challenges by designing a scalable domain decomposition method for isogeometric Stokes and mixed elasticity discretizations with continuous pressures. Our solver extends to IGA discretizations the finite element FETI-DP type preconditioner of Li and Tu [13,14], which is based on a dual–primal decomposition of the velocity/displacement and pressure unknowns in order to obtain a reduced symmetric positive definite system. Additional novelties of the present work compared with [14] are the extension to: high-order IGA discretizations (instead of low-order finite elements); more general saddle point problems with nonzero 2–2 pressure block; more general stiffness and rho-scalings operators instead of standard scaling; test with jumping coefficients across subdomain interfaces, which occur, e.g., when considering composite elastic materials. The resulting block FETI-DP preconditioner is scalable in the number of subdomains and quasi-optimal in the ratio of subdomain and element sizes, while it is sensitive to the spline polynomial degree p in case of maximal spline regularity at the subdomains interface, but it becomes robust also for increasing p when the interface regularity is reduced.

Earlier studies on non-overlapping domain decomposition algorithms for mixed elasticity and Stokes systems have focused on wirebasket and balancing Neumann–Neumann methods (see [15–19]) and on FETI-DP and BDDC methods for the incompressible limit (see [20–23,13,14]); see also [24] for BDDC preconditioners applied to different saddle point problems. Some of these studies have considered the positive definite reduction of the mixed almost incompressible elasticity system, namely, [25,18,23], using balancing Neumann–Neumann and BDDC methods (see also [26,27]) which use standard and hybrid overlapping Schwarz methods. While the positive definite reduction cannot be applied to the incompressible limit, a preconditioner for the Stokes system can still be built by using a preconditioner for a slightly compressible problem. In the more challenging case of continuous pressure approximations, FETI-DP type algorithms have been developed and analyzed in the pioneering works by Li and Tu [13,14] mentioned above. Dohrmann also has a version of the algorithm of [26] which performs virtually the same for discontinuous and continuous pressure approximations; a supporting theory is so far lacking.

The other main family of domain decomposition methods, the overlapping Schwarz methods, has also been extended to saddle point problems such as the mixed elasticity and Stokes systems by Klawonn and Pavarino [28,29]. These algorithms have been used, e.g., in computational fluid dynamics [30,31], fluid–structure interaction [32] and isogeometric analysis [7]. Earlier work by Fischer [33] studied overlapping Schwarz methods for the pressure operator of the incompressible Navier–Stokes system discretized with spectral elements. A theoretical analysis of overlapping Schwarz methods for a positive definite reformulation of almost incompressible elasticity has been recently presented in [34].

The rest of this paper is organized as follows. The Stokes and almost incompressible elasticity systems are introduced in Section 2 and discretized by NURBS-based IGA in Section 3. The FETI-DP reduced system and preconditioner are introduced in Section 4 and studied numerically in two dimensions in Section 5.

2. The Stokes and almost incompressible elasticity systems

Let Ω be a polygonal domain in $\mathbb{R}^d$, $d = 2, 3$, decomposed into N non-overlapping subdomains Ω_i of diameter H_i, and forming a coarse finite element partition τ_H of Ω,

$$\overline{\Omega} = \bigcup_{i=1}^{N} \overline{\Omega}_i. \tag{1}$$

Let $H = \max_i H_i$ be the characteristic diameter of the subdomains and $\partial\Omega_D$ a non-empty subset of $\partial\Omega$. The interface of the domain decomposition (1) is given by

$$\Gamma = \left(\bigcup_{i=1}^{N} \partial\Omega_i \right) \setminus \partial\Omega_D.$$

In the next subsection, we will further partition each subdomain into many shape-regular finite elements. We will assume that the nodes match across the interface between the subdomains.

In the following, we will use the standard notation $L^2(\Omega)$ to denote the space of square Lebesgue integrable functions on the open set Ω, and $H^1(\Omega)$ to denote the classical Sobolev space of order 1 of functions that are in $L^2(\Omega)$ with (weak) derivatives in $L^2(\Omega)$.

We assume that the boundary $\partial\Omega$ is split into two non-overlapping parts $\partial\Omega_D$ and $\partial\Omega_N$. We consider two given loading functions $\mathbf{g} \in [L^2(\Omega)]^d$ and $\mathbf{g}_N \in [L^2(\partial\Omega_N)]^d$, and the spaces

$$\mathbf{V} := \{\mathbf{v} \in H^1(\Omega)^d : \mathbf{v}|_{\partial\Omega_D} = 0\}, \quad Q := L^2(\Omega),$$

(or $Q = L^2_0(\Omega) = \{q \in L^2(\Omega) : \int_\Omega q\, dx = 0\}$ in the case $\partial\Omega_D = \partial\Omega$). We will consider the following two classical examples of saddle point problems.

The Stokes system. We consider first the Stokes problem for an incompressible fluid with viscosity μ: find the fluid velocity $\mathbf{u} \in \mathbf{V}$ and pressure $p \in Q$ such that

$$\begin{cases} \displaystyle\int_\Omega \mu\, \nabla\mathbf{u} : \nabla\mathbf{v}\, dx - \int_\Omega \operatorname{div}\mathbf{v}\, p\, dx = \langle \mathbf{f}, \mathbf{v}\rangle \ \ \forall \mathbf{v} \in \mathbf{V}, \\ \displaystyle -\int_\Omega \operatorname{div}\mathbf{u}\, q\, dx = 0 \qquad \forall q \in Q, \end{cases} \tag{2}$$

where

$$\langle \mathbf{f}, \mathbf{v}\rangle = \int_\Omega \mathbf{g}\,\mathbf{v}\, dx + \int_{\partial\Omega_N} \mathbf{g}_N\,\mathbf{v}\, dx \qquad \forall \mathbf{v} \in [H^1(\Omega)]^d. \tag{3}$$

Mixed formulation of almost incompressible linear elasticity. We consider a mixed formulation of linear elasticity for almost incompressible materials as, e.g., in [35, Ch. 1]: find the material displacement $\mathbf{u} \in \mathbf{V}$ and pressure $p \in Q$ such that

$$\begin{cases} \displaystyle 2\int_\Omega \mu\, \boldsymbol{\varepsilon}(\mathbf{u}) : \boldsymbol{\varepsilon}(\mathbf{v})\, dx - \int_\Omega \operatorname{div}\mathbf{v}\, p\, dx = \langle \mathbf{f}, \mathbf{v}\rangle \ \ \forall \mathbf{v} \in \mathbf{V}, \\ \displaystyle -\int_\Omega \operatorname{div}\mathbf{u}\, q\, dx - \int_\Omega \frac{1}{\lambda}\, pq\, dx = 0 \qquad \forall q \in Q. \end{cases} \tag{4}$$

Here $\boldsymbol{\varepsilon}$ is the symmetric gradient operator and $\mu(x)$, $\lambda(x)$ are the Lamé parameters of the material that, for simplicity, are assumed to be constant in each subdomain Ω_i, i.e. $\mu = \mu_i$ and $\lambda = \lambda_i$ in Ω_i. These parameters can be expressed in terms of the local Poisson ratio ν_i and Young's modulus E_i as

$$\mu_i := \frac{E_i}{2(1+\nu_i)}, \qquad \lambda_i := \frac{E_i\,\nu_i}{(1+\nu_i)(1-2\nu_i)}. \tag{5}$$

The material of a subdomain approaches the incompressible limit when $\nu_i \to 1/2$. Factoring out the constants μ_i and $\frac{1}{\lambda_i}$, we can define local bilinear forms in terms of integrals over the subdomains Ω_i and obtain

$$a(\mathbf{u}, \mathbf{v}) = \sum_{i=1}^N \mu_i a_i(\mathbf{u}, \mathbf{v}) := \begin{cases} \displaystyle\sum_{i=1}^N \mu_i \int_{\Omega_i} \nabla\mathbf{u} : \nabla\mathbf{v}\, dx & \text{(Stokes)} \\ \displaystyle 2\sum_{i=1}^N \mu_i \int_{\Omega_i} \varepsilon(\mathbf{u}) : \varepsilon(\mathbf{v})\, dx & \text{(mixed elasticity),} \end{cases} \tag{6}$$

$$b(\mathbf{v}, q) = \sum_{i=1}^N b_i(\mathbf{v}, q) := -\sum_{i=1}^N \int_{\Omega_i} \operatorname{div}\mathbf{v}\, q\, dx, \tag{7}$$

$$c(p, q) = \sum_{i=1}^N \frac{1}{\lambda_i} c_i(p, q) := \sum_{i=1}^N \frac{1}{\lambda_i} \int_{\Omega_i} p\, q\, dx, \qquad (c(p, q) = 0 \text{ for Stokes}). \tag{8}$$

Thus, the global Stokes and mixed elasticity problems (2) and (4) can be obtained by assembling contributions to the bilinear forms from those of the subdomains, obtaining the saddle point problem: find $\mathbf{u} \in \mathbf{V}$, $p \in Q$ such that

$$\begin{cases} a(\mathbf{u}, \mathbf{v}) + b(\mathbf{v}, p) = \langle \mathbf{f}, \mathbf{v} \rangle & \forall \mathbf{v} \in \mathbf{V}, \\ b(\mathbf{u}, q) - c(p, q) = 0 & \forall q \in Q. \end{cases} \tag{9}$$

3. NURBS-based IGA

Non-Uniform Rational B-splines (NURBS) are a standard tool for describing and modeling curves and surfaces in computer aided design and computer graphics (see e.g. [36] for an extensive description of these functions and their properties). In IGA, introduced by Hughes et al. [1] (see also [2]), NURBS are used as discretization space for the analysis of PDEs. In this section, we present a short description of B-splines, NURBS, the basics of IGA and an introduction to the proposed discretization method.

3.1. B-splines

B-splines in the plane are piecewise polynomial curves composed of linear combinations of B-spline basis functions. A *knot vector* is a set of non-decreasing real numbers representing coordinates in the parametric space of the curve

$$\{\xi_1 = 0, \ldots, \xi_{n+p+1} = 1\}, \tag{10}$$

where p is the polynomial degree of the B-spline and n is the number of basis functions (and control points) necessary to describe it. The interval (ξ_1, ξ_{n+p+1}) is called a *patch*. A knot vector is said to be *uniform* if its knots are uniformly-spaced and *non-uniform* otherwise. The maximum allowed knot multiplicity is $p + 1$; a knot vector is said to be *open* if its first and last knots have multiplicity $p+1$. In what follows, we always employ open knot vectors. Basis functions formed from open knot vectors are interpolatory at the ends of the parametric interval $\widehat{I} := (0, 1)$, but they are not, in general, interpolatory at interior knots.

Given a knot vector, univariate B-spline basis functions are defined recursively starting with $p = 0$ (piecewise constants)

$$N_i^0(\xi) = \begin{cases} 1 & \text{if } \xi_i \le \xi < \xi_{i+1} \\ 0 & \text{otherwise.} \end{cases} \tag{11}$$

For $p > 1$:

$$N_i^p(\xi) = \begin{cases} \dfrac{\xi - \xi_i}{\xi_{i+p} - \xi_i} N_i^{p-1}(\xi) + \dfrac{\xi_{i+p+1} - \xi}{\xi_{i+p+1} - \xi_{i+1}} N_{i+1}^{p-1}(\xi) & \text{if } \xi_i \le \xi < \xi_{i+p+1} \\ 0 & \text{otherwise,} \end{cases} \tag{12}$$

where, in (12), we adopt the convention $0/0 = 0$. Thus, the general basis function N_i^p has support

$$\Theta_i := \operatorname{supp}(N_i^p) = (\xi_i, \xi_{i+p+1}), \qquad i = 1, 2, \ldots, n.$$

The functions N_i^p form a *partition of unity*, as shown in [36]. If internal knots are not repeated, B-spline basis functions are C^{p-1}-continuous. If a knot has multiplicity α, the basis is C^k-continuous, with $k = p-\alpha$, at that knot. In particular, when a knot has multiplicity $\alpha = p$, the basis is C^0 and interpolates the control point at that location. In the following, we will assume that the maximum knot multiplicity is p so that all considered functions will be (at least) globally continuous. We define the spline space

$$\widehat{\mathcal{S}}_h = \operatorname{span}\{N_i^p(\xi), i = 1, \ldots, n\}. \tag{13}$$

By means of tensor products, a multi-dimensional B-spline region can be constructed. We discuss here the case of a two-dimensional region, the higher-dimensional case being analogous. Let $\widehat{\Omega} := (0, 1) \times (0, 1)$ be the two-dimensional parametric space. Consider the knot vectors $\{\xi_1 = 0, \ldots, \xi_{n+p+1} = 1\}$ and $\{\eta_1 = 0, \ldots, \eta_{m+q+1} = 1\}$, and an $n \times m$

net of control points $\mathbf{C}_{i,j}$. One dimensional basis functions N_i^p and M_j^q (with $i = 1, \ldots, n$ and $j = 1, \ldots, m$) of degree p and q, respectively, are defined from the knot vectors. The bivariate spline basis on $\widehat{\Omega}$ is then defined by the tensor product construction

$$B_{i,j}^{p,q}(\xi, \eta) = N_i^p(\xi) M_j^q(\eta).$$

Observe that the two knot vectors $\{\xi_1 = 0, \ldots, \xi_{n+p+1} = 1\}$ and $\{\eta_1 = 0, \ldots, \eta_{m+q+1} = 1\}$ generate a mesh of rectangular elements in the parametric space in a natural way. Analogous to (13), we define

$$\widehat{\mathcal{S}}_h = \text{span}\{B_{i,j}^{p,q}(\xi, \eta),\ i = 1, \ldots, n,\ j = 1, \ldots, m\}. \tag{14}$$

3.2. NURBS maps and spaces

In general, a rational B-spline in $\mathbb{R}^d$ is the projection onto d-dimensional physical space of a polynomial B-spline defined in $(d + 1)$-dimensional homogeneous coordinate space. For a complete discussion, see the book [36] and references therein. In this way, a great variety of geometrical entities can be constructed and, in particular, all conic sections in physical space can be obtained exactly. To obtain a NURBS curve in $\mathbb{R}^2$, we start by introducing the NURBS basis functions of degree p

$$R_i^p(\xi) = \frac{N_i^p(\xi)\omega_i}{\sum_{\hat{\imath}=1}^{n} N_{\hat{\imath}}^p(\xi)\omega_{\hat{\imath}}} = \frac{N_i^p(\xi)\omega_i}{w(\xi)}, \tag{15}$$

where the denominator $w(\xi) = \sum_{\hat{\imath}=1}^{n} N_{\hat{\imath}}^p(\xi)\omega_{\hat{\imath}} \in \widehat{\mathcal{S}}_h$ is called the weight function.

The NURBS curve is then defined by

$$\mathbf{C}(\xi) = \sum_{i=1}^{n} R_i^p(\xi)\mathbf{C}_i, \tag{16}$$

where $\mathbf{C}_i \in \mathbb{R}^2$ are known as control points.

Analogously to B-splines, NURBS basis functions on the two-dimensional parametric space $\widehat{\Omega} = (0, 1) \times (0, 1)$ are defined as

$$R_{i,j}^{p,q}(\xi, \eta) = \frac{B_{i,j}^{p,q}(\xi, \eta)\omega_{i,j}}{\sum_{\hat{\imath}=1}^{n}\sum_{\hat{\jmath}=1}^{m} B_{\hat{\imath},\hat{\jmath}}^{p,q}(\xi, \eta)\omega_{\hat{\imath},\hat{\jmath}}} = \frac{B_{i,j}^{p,q}(\xi, \eta)\omega_{i,j}}{w(\xi, \eta)}, \tag{17}$$

where $\omega_{i,j} = (\mathbf{C}_{i,j}^{\omega})_3$ and the denominator is the weight function denoted also by $w(\xi, \eta)$. Observe that the continuity and support of NURBS basis functions are the same as for B-splines. NURBS spaces are the span of the basis functions (17).

NURBS regions are defined in terms of the basis functions (17). In particular a *single-patch* domain Ω is a NURBS region associated with the $n \times m$ net of control points $\mathbf{C}_{i,j}$. We then introduce the geometrical map $\mathbf{F} : \widehat{\Omega} \to \Omega$ given by

$$\mathbf{F}(\xi, \eta) = \sum_{i=1}^{n}\sum_{j=1}^{m} R_{i,j}^{p,q}(\xi, \eta)\mathbf{C}_{i,j}, \tag{18}$$

and following the isoparametric approach, the space of NURBS scalar fields on the domain Ω is defined, component by component as the span of the *push-forward* of the basis functions (17)

$$\mathcal{N}_h := \text{span}\{R_{i,j}^{p,q} \circ \mathbf{F}^{-1},\ \text{with } i = 1, \ldots, n;\ j = 1, \ldots, m\}. \tag{19}$$

The image of the elements in the parametric space are elements in the physical space. The physical mesh on Ω is therefore

$$\mathcal{T}_h = \left\{ \mathbf{F}((\xi_i, \xi_{i+1}) \times (\eta_j, \eta_{j+1})), \text{ with } i = 1, \ldots, n+p, \ j = 1, \ldots, m+q \right\}, \tag{20}$$

where the empty elements are not considered.

3.3. Isogeometric discretization of the Stokes and mixed elasticity problems

We are now able to present the isogeometric approximation of the Stokes and mixed elasticity problems (2) and (4). In the present description we consider, for simplicity of exposition, only the homogeneous Dirichlet case $\partial\Omega_D = \partial\Omega$. As observed for instance in [37], in order to obtain spaces with homogeneous Dirichlet boundary conditions it is sufficient to eliminate the first and last function in each coordinate. We therefore introduce the spline space (for instance in two dimensions) living in parameter space

$$\widehat{\mathbf{V}}_h = [\widehat{\mathcal{S}}_h \cap H_0^1(\widehat{\Omega})]^d = [\text{span}\{B_{i,j}^{p,q}(\xi, \eta), \ i = 2, \ldots, n-1, \ j = 2, \ldots, m-1\}]^d$$

and the NURBS space living in physical space

$$\mathbf{V}_h = [\mathcal{N}_h \cap H_0^1(\Omega)]^d = [\text{span}\{R_{i,j}^{p,q} \circ \mathbf{F}^{-1}, \text{ with } i = 2, \ldots, n-1; \ j = 2, \ldots, m-1\}]^d. \tag{21}$$

In order to discretize our saddle point problems, we need a proper coupling between the mapped NURBS velocity/displacement space $\mathbf{V}_h$ and the pressure space Q_h, see [35]. Here we consider the following pair of spaces based on isogeometric Taylor–Hood elements introduced in [12], that have proved to be inf–sup stable. The space $\mathbf{V}_h$ is built as in (21), but with the restrictions that

- the polynomial degrees satisfy $p \geq 2$ and $q \geq 2$;
- all the knots are repeated at least twice, and therefore the space is at most $C^{p-2} - C^{q-2}$ regular across mesh lines.

The space Q_h is built as the span

$$Q_h = \text{span}\{\mathsf{R}_{i,j}^{p-1,q-1} \circ \mathbf{F}^{-1}, \text{ with } i = 1, \ldots, \bar{n}; \ j = 1, \ldots, \bar{m}\} \cap L_0^2(\Omega), \tag{22}$$

where the basis $\mathsf{R}_{i,j}^{p-1,q-1}$ is generated from the same knot vectors used for the $\mathbf{V}_h$ space, but with one *less* repetition per multiple knot. Therefore, the space Q_h of pressures turns out to have the same regularity across mesh lines as $\mathbf{V}_h$, but one less polynomial degree. In the simple case of equal polynomial degree $p = q$ along each coordinate, we will then consider isogeometric Taylor–Hood elements with velocity/displacement basis functions of degree p, regularity $p-2$ and pressure basis functions of degree $p-1$, regularity $p-2$.

The IGA approximation of our model Stokes or mixed elasticity problem (9) now reads: find $\mathbf{u}_h \in \mathbf{V}_h$, $p_h \in Q_h$ such that

$$\begin{cases} a(\mathbf{u}_h, \mathbf{v}_h) + b(\mathbf{v}_h, p_h) = \langle \mathbf{f}, \mathbf{v}_h \rangle & \forall \mathbf{v}_h \in \mathbf{V}_h, \\ b(\mathbf{u}_h, q_h) - c(p_h, q_h) = 0 & \forall q_h \in Q_h. \end{cases} \tag{23}$$

Denoting with the same symbols $\mathbf{u}_h$, p_h both the isogeometric functions and their vector representations in the isogeometric basis, the matrix form of system (23) is

$$\begin{bmatrix} A & B^T \\ B & -C \end{bmatrix} \begin{bmatrix} \mathbf{u}_h \\ p_h \end{bmatrix} = \begin{bmatrix} \mathbf{f} \\ 0 \end{bmatrix}, \tag{24}$$

where A, B, C are the matrices associated with the bilinear forms $a(\cdot,\cdot)$, $b(\cdot,\cdot)$, $c(\cdot,\cdot)$, respectively.

The interested reader may find more details on IGA as well as many interesting applications in a number of recently published papers mentioned in the Introduction. The three-dimensional case is analogous and not discussed here.

4. Dual–primal decomposition, FETI-DP reduced system, and block FETI-DP preconditioner

4.1. Dual–primal decomposition

We follow closely [14, Sec. 3 and 4] and the notation therein; we refer to [19] for a general introduction to dual–primal domain decomposition methods. The velocity/displacement variables are split into interior (I), dual (Δ), primal (Π) components $\mathbf{u}_h = (\mathbf{u}_I, \mathbf{u}_\Delta, \mathbf{u}_\Pi)$, the pressure variables into interior (I) and interface (Γ) components $p_h = (p_I, p_\Gamma)$, and we denote by λ_Δ the Lagrange multipliers used to enforce the continuity of the dual velocities/displacements. Reordering the variables as $(\mathbf{u}_I, p_I, \mathbf{u}_\Delta, \mathbf{u}_\Pi, p_\Gamma, \lambda_\Delta)$ and splitting the matrices A and B in the appropriate blocks associated with this splitting, the original system (24) is equivalent to

$$\begin{bmatrix} A_{II} & B_{II}^T & A_{I\Delta} & A_{I\Pi} & B_{\Gamma I}^T & 0 \\ B_{II} & -C_{II} & B_{\Delta I}^T & B_{\Pi I}^T & -C_{I\Gamma} & 0 \\ A_{\Delta I} & B_{\Delta I} & A_{\Delta\Delta} & A_{\Delta\Pi} & B_{\Gamma\Delta}^T & B_\Delta^T \\ A_{\Pi I} & B_{\Pi I} & A_{\Pi\Delta} & A_{\Pi\Pi} & B_{\Gamma\Pi}^T & 0 \\ B_{\Gamma I} & -C_{\Gamma I} & B_{\Gamma\Delta} & B_{\Gamma\Pi} & -C_{\Gamma\Gamma} & 0 \\ 0 & 0 & B_\Delta & 0 & 0 & 0 \end{bmatrix} \begin{bmatrix} \mathbf{u}_I \\ p_I \\ u_\Delta \\ u_\Pi \\ p_\Gamma \\ \lambda_\Delta \end{bmatrix} = \begin{bmatrix} \mathbf{f}_I \\ 0 \\ \mathbf{f}_\Delta \\ \mathbf{f}_\Pi \\ 0 \\ 0 \end{bmatrix}. \tag{25}$$

4.2. FETI-DP reduced system

We can reduce the indefinite system (25) to a symmetric positive definite system by eliminating the $(\mathbf{u}_I, p_I, \mathbf{u}_\Delta, \mathbf{u}_\Pi)$ variables, i.e. by taking the Schur complement of A with respect to the leading 4×4 block $\widetilde{A}$ in (25) to obtain

$$G \begin{bmatrix} p_\Gamma \\ \lambda_\Delta \end{bmatrix} = g, \tag{26}$$

where

$$G = \widetilde{B}\widetilde{A}^{-1}\widetilde{B}^T + \widetilde{C}, \qquad g = \widetilde{B}\widetilde{A}^{-1} \begin{bmatrix} \mathbf{f}_I \\ 0 \\ \mathbf{f}_\Delta \\ \mathbf{f}_\Pi \end{bmatrix}, \tag{27}$$

$$\widetilde{A} = \begin{bmatrix} A_{II} & B_{II}^T & A_{I\Delta} & A_{I\Pi} \\ B_{II} & -C_{II} & B_{I\Delta} & B_{I\Pi} \\ A_{\Delta I} & B_{I\Delta}^T & A_{\Delta\Delta} & A_{\Delta\Pi} \\ A_{\Pi I} & B_{I\Pi}^T & A_{\Pi\Delta} & A_{\Pi\Pi} \end{bmatrix}, \qquad \widetilde{B} = \begin{bmatrix} B_{\Gamma I} & -C_{\Gamma I} & B_{\Gamma\Delta} & B_{\Gamma\Pi} \\ 0 & 0 & B_\Delta & 0 \end{bmatrix}, \qquad \widetilde{C} = \begin{bmatrix} C_{\Gamma\Gamma} & 0 \\ 0 & 0 \end{bmatrix}. \tag{28}$$

Analogously to the Stokes case treated in [14, Sec. 4], it can be proven that $-G$ is symmetric positive semidefinite by using Sylvester's law of inertia for the representation of G as the Schur complement of (25) with respect to the $\widetilde{C}$ block

$$\begin{bmatrix} I & 0 \\ -\widetilde{B}\widetilde{A}^{-1} & I \end{bmatrix} \begin{bmatrix} \widetilde{A} & \widetilde{B}^T \\ \widetilde{B} & -\widetilde{C} \end{bmatrix} \begin{bmatrix} I & -\widetilde{A}^{-1}\widetilde{B}^T \\ 0 & I \end{bmatrix} = \begin{bmatrix} \widetilde{A} & 0 \\ 0 & -G \end{bmatrix}.$$

The action of G on a given vector and the construction of the right-hand side g of the reduced system (27) require us to compute the action of $\widetilde{A}^{-1}$ on a given vector. As shown in [14, Sec. 4], this action can be computed by solving once a coarse problem associated to the primal variables and by twice solving independent subdomain saddle point problems with Neumann boundary conditions. Indeed, partitioning $\widetilde{A}$ into interior-dual and primal blocks

$$\widetilde{A} = \begin{bmatrix} A_{rr} & A_{\Pi r}^T \\ A_{\Pi r} & A_{\Pi\Pi} \end{bmatrix}, \quad \text{where } A_{rr} = \begin{bmatrix} A_{II} & B_{II}^T & A_{I\Delta} \\ B_{II} & -C_{II} & B_{I\Delta} \\ A_{\Delta I} & B_{I\Delta}^T & A_{\Delta\Delta} \end{bmatrix}, \quad A_{\Pi r} = \begin{bmatrix} A_{\Pi I} & B_{I\Pi}^T & A_{\Pi\Delta} \end{bmatrix},$$

and defining the primal Schur complement $S_\Pi = A_{\Pi\Pi} - A_{\Pi r}A_{rr}^{-1}A_{\Pi r}^T$, we can see that the action of $\widetilde{A}^{-1}$ can be computed as

$$\begin{bmatrix} A_{rr} & A_{\Pi r}^T \\ A_{\Pi r} & A_{\Pi\Pi} \end{bmatrix}^{-1} \begin{bmatrix} v_r \\ v_\Pi \end{bmatrix} = \begin{bmatrix} A_{rr}^{-1}v_r - A_{rr}^{-1}A_{\Pi r}^T S_\Pi^{-1}(v_\Pi - A_{\Pi r}A_{rr}^{-1}v_r) \\ S_\Pi^{-1}(v_\Pi - A_{\Pi r}A_{rr}^{-1}v_r) \end{bmatrix}. \tag{29}$$

The action of S_Π^{-1} requires one solution of a coarse problem associated to the primal variables, while the action of A_{rr}^{-1} requires the solution of independent subdomain saddle point problems with Neumann boundary conditions for the dual variables; this last action has to be computed twice, once on v_r and once on the second term of the first component of (29).

4.3. Block FETI-DP preconditioner

Our isogeometric block FETI-DP preconditioner for the reduced system (26) is defined as

$$M_D^{-1} = \begin{bmatrix} M_{p_\Gamma}^{-1} & 0 \\ 0 & M_{\lambda_\Delta}^{-1} \end{bmatrix}, \tag{30}$$

where M_{p_Γ} is the mass matrix associated with the interface pressure variables p_Γ and $M_{\lambda_\Delta}^{-1}$ is the λ_Δ-block preconditioner

$$M_{\lambda_\Delta}^{-1} = B_{\Delta,D}H_\Delta B_{\Delta,D}^T.$$

Here H_Δ is the direct sum of the local discrete harmonic extension operators $H_\Delta^{(i)}$, $i = 1, \ldots, N$, each defined by solving a local elliptic problem on subdomain Ω_i

$$\begin{bmatrix} A_{II}^{(i)} & A_{I\Delta}^{(i)} \\ A_{\Delta I}^{(i)} & A_{\Delta\Delta}^{(i)} \end{bmatrix} \begin{bmatrix} \mathbf{u}_I^{(i)} \\ \mathbf{u}_\Delta^{(i)} \end{bmatrix} = \begin{bmatrix} 0 \\ H_\Delta^{(i)}\mathbf{u}_\Delta^{(i)} \end{bmatrix} \tag{31}$$

with given boundary velocity $\mathbf{u}_\Delta^{(i)}$ and zero primal velocities $\mathbf{u}_\Pi^{(i)} = 0$. The scaling operator

$$B_{\Delta,D} = \begin{bmatrix} D_\Delta B_\Delta^{(1)} & D_\Delta B_\Delta^{(2)} & \ldots & D_\Delta B_\Delta^{(N)} \end{bmatrix}$$

is defined by scaling the boolean matrix $B_\Delta = \begin{bmatrix} B_\Delta^{(1)} & B_\Delta^{(2)} & \ldots & B_\Delta^{(N)} \end{bmatrix}$ which enforces the continuity constraint $B_\Delta \boldsymbol{w}_\Delta = 0$ for the dual velocity degrees of freedom $\boldsymbol{w}_\Delta$ shared by neighboring subdomains. D_Δ is a diagonal matrix with scaling coefficients $\delta^\dagger(x)$ chosen as in FETI-DP and BDDC methods. In particular, we will consider the two choices known as ρ-scaling and stiffness scaling, defined as follows.

4.4. Diagonal scaling

For each subdomain Ω_i and node x_j associated with the jth component of the dual vector $\mathbf{u}_\Delta$, letting $\mathcal{N}_j = \{\ell : \Omega_\ell \cap \text{supp}(B_j^{p,q}) \neq \emptyset\}$, we define:

$$\rho\text{-scaling:} \quad \delta_j^{(i)^\dagger} = \mu_i / \Big(\sum_{\ell \in \mathcal{N}_j} \mu_\ell \Big), \tag{32}$$

where μ_ℓ is the value of the viscosity or Lamé parameter μ on Ω_ℓ, assumed for simplicity constant on each subdomain (in the case of a constant viscosity coefficient μ on all of Ω, for the bi-variate case all the $\delta_j^{(i)^\dagger}$ above are equal to $1/2$ while in the tri-variate case they equal $1/2$ for subdomain edge nodes and $1/4$ for vertex nodes);

$$\text{stiffness scaling:} \quad \delta_j^{(i)^\dagger} = a_i(B_j^{p,q}, B_j^{p,q}) / \Big(\sum_{\ell \in \mathcal{N}_j} a_\ell(B_j^{p,q}, B_j^{p,q}) \Big), \tag{33}$$

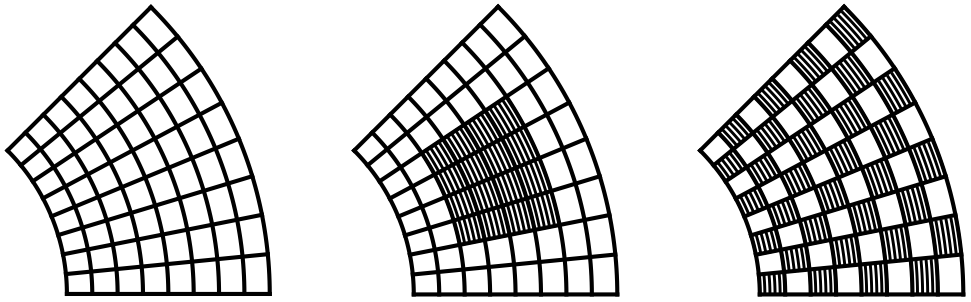

Fig. 1. Left: ring-sector NURBS domain subdivided into 8×8 subdomains; center and right: ring-sector NURBS domains in the central jump and checkerboard tests.

where $a_i(\cdot,\cdot)$ is the restriction of the bilinear form $a(\cdot,\cdot)$ to the domain Ω_i (analogously for $a_\ell(\cdot,\cdot)$). The obvious analogous scalings are defined in the case of NURBS basis functions.

We remark that the proper extension to saddle point problems of the powerful deluxe scaling, that we studied in [10] for IGA discretizations of scalar elliptic problems, is still an open problem.

4.5. Convergence rate estimate

The finite element proof in [14, Th. 7.6] of a scalable condition number bound for the preconditioned operator $M_D^{-1}G$ can be extended to our isogeometric context, to obtain:

Theorem 4.1. *If the coarse space is spanned by the subdomain fat vertex velocity/displacement basis functions in 2D and by the subdomain fat vertex and fat edge velocity/displacement basis functions in 3D, then there exist positive constants c, C_1, C_2 independent of h, H, N (but not of p, k) such that*

$$\frac{c\beta^2}{1+\beta^2} x^T M_D x \leq x^T G x \leq \left(C_1 + C_2 \Phi\Big(\frac{H}{h}\Big)\right) x^T M_D x,$$

where β is the inf–sup constant of the isogeometric Taylor–Hood mixed elements considered and

$$\Phi\Big(\frac{H}{h}\Big) = \begin{cases} (1+\log(H/h))^2 & \text{for } \rho\text{-scaling}, \\ (H/h)(1+\log(H/h))^2 & \text{for stiffness-scaling}. \end{cases}$$

The proofs of the lower and upper bounds follow mostly the same algebraic steps of [14, Th. 7.6]. The only substantial difference is the extension to our isogeometric context of the edge lemma required in [14, Lemma 6.2], which then yields [14, Lemma 7.2] and finally the upper bound of [14, Th. 7.6]. Such isogeometric edge lemma has been proven in [5, Th. 6.1 and 6.2] for the 2D case with coarse space spanned by the subdomain fat vertex velocity/displacement basis functions; see also [10, Th. 4.3 and 4.4] for the use of such edge lemma in the analysis of isogeometric BDDC algorithms with deluxe scaling. The 3D case requires analogous isogeometric edge and face lemmas for coarse spaces spanned by subdomain fat vertex and fat edge velocity/displacement basis functions. To our knowledge, such 3D isogeometric lemmas have not been explicitly proven yet, but we conjecture that they can be obtained by extending to the 3D case the fairly technical 2D tools of [5, Th. 6.1 and 6.2].

5. Numerical results

In this section, we study the convergence properties of the isogeometric block FETI-DP preconditioner for the Stokes and almost incompressible elasticity (AIE) problems on 2D physical NURBS domains illustrated in Figs. 1 and 3. Mixed homogeneous Dirichlet–Neumann boundary conditions are imposed. The problem is discretized by isogeometric NURBS spaces with an associated mesh size h, polynomial degree p, regularity k, using the Matlab isogeometric library GeoPDEs [38]. We recall that, in all the following tests, p will denote the polynomial degree of the pressure space and k will always be the maximal regularity, thus $k = p - 1$. The polynomial degree and regularity of velocity or displacement space are $p + 1$ and k, respectively, according to the definition of

Table 1
Stokes system. FETI-DP PCG in ring-sector domain: condition number *cond* and iteration counts it. as a function of the number of subdomains N and mesh size $1/h$ for $p = 2,\ k = 1$ (pressure) and $p = 3,\ k = 1$ (velocity) NURBS, $k_\Gamma = 1$.

ρ-scaling										
N	$1/h = 8$		$1/h = 16$		$1/h = 32$		$1/h = 64$		$1/h = 128$	
	cond	it.	*cond*	it.	*cond*	it.	*cond*	it.	*cond*	it.
2×2	6.99	21	8.36	21	9.76	21	11.28	21	12.99	21
4×4			8.84	25	10.63	27	12.38	29	14.38	30
8×8					9.69	27	11.46	29	13.38	31
16×16							10.18	27	11.83	29
32×32									10.45	28
Stiffness-scaling										
2×2	7.40	19	10.63	20	17.17	20	31.31	23	65.48	30
4×4			8.96	25	12.47	27	19.21	31	39.26	38
8×8					9.61	26	12.92	28	19.90	32
16×16							10.08	27	12.95	29
32×32									10.30	27

the generalized Taylor–Hood isogeometric elements introduced in [12]. The domain is decomposed into N non-overlapping subdomains of characteristic size H. In all the numerical tests reported in the following, the FETI-DP coarse space is spanned by the subdomain fat vertex velocity/displacement basis functions. We will denote by k_Γ the regularity of the spline functions at the interface between the subdomains. k_Γ might coincide with the regularity k of the space or be lower, yielding a smaller interface problem (26). The reduced linear system (26) arising from the isogeometric discretization is solved by the Preconditioned Conjugate Gradient (PCG) method preconditioned by the block FETI-DP preconditioner (30). We employ a zero initial guess and a stopping criterion of 10^{-8} reduction of the relative residual.

In the following tests, we study how the convergence rate of the proposed method depends on the discretization parameters h, p, k, the number of subdomains N, the domain deformation and the jumps of the elastic coefficients E and ν across subdomain boundaries.

5.1. Stokes system: FETI-DP scalability in N and quasi-optimality in H/h

We consider here the Stokes equations on the ring-sector NURBS domain shown in Fig. 1. The condition number (*cond*), defined as the ratio of the extreme eigenvalues of the FETI-DP preconditioned operator and PCG iteration counts (it.) as a function of the number of subdomains N and mesh size $1/h$ are reported in Table 1 for $p = 2,\ k = 1$ (pressure), $p = 3,\ k = 1$ (velocity) NURBS spaces and regularity $k_\Gamma = 1$; in Table 2 for $p = 3,\ k = 2$ (pressure), $p = 4,\ k = 2$ (velocity) NURBS spaces and $k_\Gamma = 2$; in Table 3 for $p = 3,\ k = 2$ (pressure), $p = 4,\ k = 2$ (velocity) NURBS spaces and $k_\Gamma = 1$. In all cases, both ρ-scaling and stiffness scaling are considered. The blank entries in the lower triangular part of these tables correspond to cases where the ratio H/h is so small that there are no interior pressure degrees of freedom in the local problems and we cannot build our FETI-DP reduced system (26). The results show that the proposed preconditioner is scalable, since moving along the diagonals of the tables the condition number is bounded from above by a constant independent of N, see also Fig. 2 (left). The plots in Fig. 2 (right) also confirm the main bound of Theorem 4.1: with ρ-scaling, the condition numbers seem to grow as $\log^2(H/h)$, whereas, with stiffness-scaling, the growth in H/h is super-linear. For high interface regularity $k_\Gamma = 2$ (Table 2) and small H/h ratio, the ρ-scaling behaves much worse than stiffness-scaling, as already observed in our previous paper [5] in the case of BDDC preconditioners applied to isogeometric discretizations of scalar elliptic problems.

5.2. Stokes system: FETI-DP dependence on spline polynomial degree p

In this test, we study the behavior of the FETI-DP preconditioner with respect to the spline polynomial degree p, the regularity k and the subdomains interface regularity k_Γ. We recall that our theory does not cover the dependence of the FETI-DP preconditioner on these parameters. The problem considered is the Stokes system on the ring-sector domain. As in the previous test, p and $k = p - 1$ denote the parameters of the pressure space, while the velocities

Table 2
Stokes system. FETI-DP PCG in ring-sector domain: condition number *cond* and iteration counts it. as a function of the number of subdomains N and mesh size $1/h$ for $p = 3,\ k = 2$ (pressure) and $p = 4,\ k = 2$ (velocity) NURBS, $k_\Gamma = 2$.

ρ-scaling										
N	$1/h = 8$		$1/h = 16$		$1/h = 32$		$1/h = 64$		$1/h = 128$	
	cond	it.	*cond*	it.	*cond*	it.	*cond*	it.	*cond*	it.
2×2	94.11	63	100.11	72	102.57	75	103.52	75	103.85	74
4×4			110.85	86	106.55	84	104.89	85	103.16	82
8×8					116.09	94	108.03	89	105.22	88
16×16							119.90	97	108.80	93
32×32									121.14	99
Stiffness-scaling										
2×2	18.48	28	18.96	31	41.38	36	94.56	40	215.95	50
4×4			20.15	36	21.32	39	49.90	50	118.52	63
8×8					20.08	38	22.07	40	53.71	55
16×16							19.86	39	22.31	41
32×32									19.94	39

Table 3
Stokes system. FETI-DP PCG in ring-sector domain: condition number *cond* and iteration counts it. as a function of the number of subdomains N and mesh size $1/h$ for $p = 3,\ k = 2$ (pressure) and $p = 4,\ k = 2$ (velocity) NURBS, $k_\Gamma = 1$.

ρ-scaling										
N	$1/h = 8$		$1/h = 16$		$1/h = 32$		$1/h = 64$		$1/h = 128$	
	cond	it.	*cond*	it.	*cond*	it.	*cond*	it.	*cond*	it.
2×2	7.77	21	9.13	22	10.61	21	12.26	21	14.10	20
4×4			9.94	27	11.64	28	13.44	30	15.86	31
8×8					10.65	28	12.53	30	14.54	32
16×16							11.05	29	12.88	30
32×32									11.32	29
Stiffness-scaling										
2×2	8.14	20	10.65	20	15.18	20	24.22	22	44.45	25
4×4			10.09	26	12.87	28	17.94	32	29.52	36
8×8					10.64	27	13.39	29	18.81	33
16×16							10.87	28	13.55	30
32×32									11.14	29

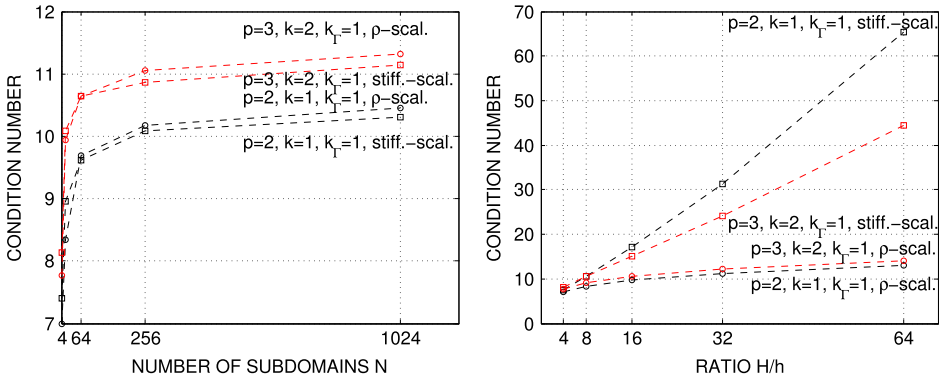

Fig. 2. Stokes system. Plots from Tables 1 and 3.

Table 4
Stokes system. FETI-DP PCG with stiffness scaling in ring-sector domain: condition number *cond*, maximum and minimum eigenvalues λ_{max}, λ_{min}, iteration counts it. as a function of the spline polynomial degree p, for different choices of interface regularity $k_\Gamma = p-1, 2, 1, 0$. Fixed fine mesh $1/h = 64$, subdomains mesh $1/H = 4$.

Stiffness-scaling

p	$k_\Gamma = p-1$				$k_\Gamma = 2$			
	cond	λ_{max}	λ_{min}	it.	*cond*	λ_{max}	λ_{min}	it.
2	19.31	7.17	3.73e−1	31	–	–	–	–
3	49.90	17.69	3.54e−1	50	49.90	17.69	3.54e−1	50
4	47.25	17.20	3.64e−1	60	54.76	19.07	3.48e−1	50
5	125.89	44.12	3.50e−1	89	58.22	20.07	3.45e−1	55
6	526.04	188.72	3.59e−1	155	61.06	20.92	3.43e−1	55
7	3162.63	1093.36	3.46e−1	299	64.09	21.87	3.41e−1	60
8	7600.48	2685.69	3.53e−1	467	66.80	22.73	3.40e−1	61
p	$k_\Gamma = 1$				$k_\Gamma = 0$			
	cond	λ_{max}	λ_{min}	it.	*cond*	λ_{max}	λ_{min}	it.
2	19.31	7.17	3.73e−1	31	18.26	6.58	3.60e−1	32
3	17.94	6.56	3.66e−1	32	19.99	7.22	3.61e−1	33
4	17.52	6.36	3.63e−1	32	21.37	7.74	3.62e−1	33
5	17.53	6.35	3.62e−1	31	22.53	8.17	3.63e−1	35
6	17.84	6.46	3.62e−1	32	23.54	8.55	3.63e−1	36
7	18.25	6.61	3.62e−1	33	24.43	8.89	3.64e−1	37
8	18.71	6.78	3.62e−1	34	25.23	9.19	3.64e−1	37

belong to the $p+1$, $p-1$ NURBS space. The ring-sector domain is discretized by a mesh of size $h = 1/64$, subdivided into $N = 4 \times 4$ subdomains, while p increases from 2 to 8. Inside the subdomains k is always maximal, i.e. $k = p-1$, while on the interface k_Γ is equal to $k = p-1, 2$ (top), 1 and 0 (bottom). Stiffness-scaling is employed in all the cases. The results reported in Table 4 show that, when k_Γ is maximal, the FETI-DP preconditioner behaves well only for $p = 2, 3, 4$ and then starts to degenerate. Instead, for k_Γ equal to 2 or 0 the growth of the condition number seems to be logarithmic in p. For $k_\Gamma = 1$, the behavior is less clear, since the condition numbers initially decreases and then increases very slowly with p. The reason of the sub-optimal behavior for $p \geq 5$ and maximal interface regularity $k_\Gamma = p-1$ could be attributed to the non-optimal choice of scaling functions, as observed in our previous isogeometric BDDC paper [5] for scalar elliptic problems. A possible remedy could be the use of deluxe scaling functions, see e.g. [10], but the extension of deluxe scaling to saddle point problems is still an open problem even for standard finite element discretizations.

5.3. Stokes system: FETI-DP dependence on NURBS domain deformation

The table in the middle of Fig. 3 shows the performance of FETI-DP PCG without preconditioner (left columns) and with preconditioner with ρ-scaling (middle columns) and with stiffness scaling (right columns) for four increasingly deformed NURBS domains A, B, C, D (top). The discretization parameters are $p = 2, k = 1, 1/h = 32, 1/H = 4$. The lower panels of the figure shows the convergence history of FETI-DP PCG without preconditioner (bottom left) and with preconditioner (bottom right). The results show that the increasing deformations severely worsen the unpreconditioned CG convergence rate, which deteriorates from 714 iterations for domain A to 3108 iterations for the severely deformed domain D, with a highly oscillatory convergence history in all cases. The preconditioned FETI-DP algorithm is still sensitive to the domain deformation but it performs much better, passing from 29 iterations for domain A to 75 iterations for domain D (when ρ-scaling is used) or from 30 iterations for domain A to 102 iterations for domain D (when stiffness-scaling is used). The results of the Table indicate that for both unpreconditioned and preconditioned FETI-DP algorithm the deformation affects mostly the largest eigenvalue λ_{max}, while the smallest eigenvalue λ_{min} is almost unchanged. In all tests, ρ-scaling performs better than stiffness-scaling, reducing the condition number of the unpreconditioned operator in the hardest test with domain D of about 5 order of magnitude (from $2.8 \cdot 10^7$ to 249.83) and reducing the iterations of about a factor 40 (from 3108 to 75).

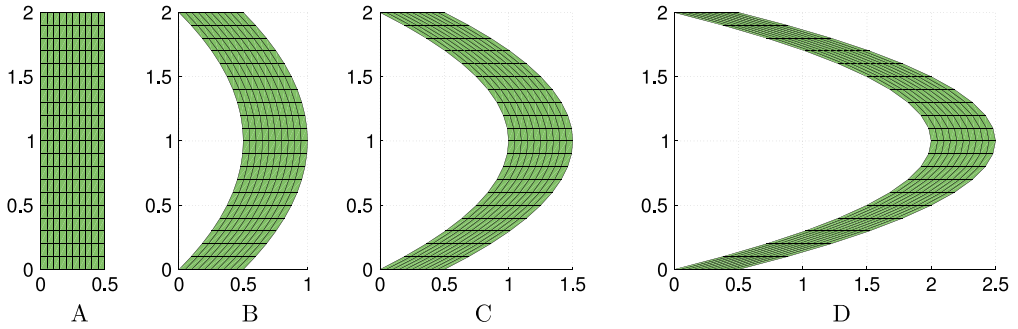

	unpreconditioned CG				ρ-scaling				stiffness-scaling			
	cond	λ_{max}	λ_{min}	it.	*cond*	λ_{max}	λ_{min}	it.	*cond*	λ_{max}	λ_{min}	it.
A	5.11e+6	79.61	1.56e-5	715	14.52	5.52	3.80e-1	29	16.88	6.30	3.73e-1	30
B	6.40e+6	86.54	1.35e-5	1107	20.16	7.38	3.66e-1	33	23.85	8.78	3.68e-1	37
C	1.03e+7	139.56	1.35e-5	1661	46.87	18.18	3.88e-1	40	58.54	23.23	3.97e-1	48
D	2.80e+7	380.36	1.35e-5	3108	249.83	108.70	4.35e-1	75	358.43	163.64	4.56e-1	102

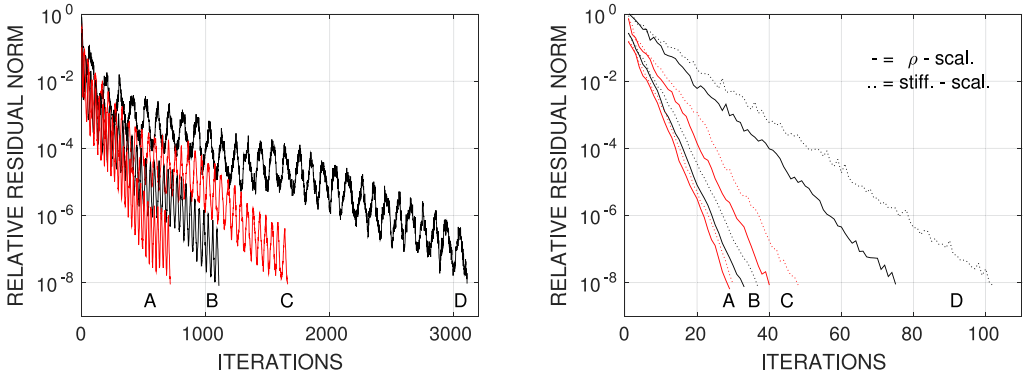

Fig. 3. Stokes system, $p = 2$, $k = 1$, $1/h = 32$, $1/H = 4$. Top: increasingly deformed NURBS domains A, B, C, D. Bottom: convergence history of FETI-DP PCG without preconditioner (left) and with preconditioner (right).

5.4. AIE system: FETI-DP scalability in N and quasi-optimality in H/h

We then consider in Table 5 the AIE equations on the ring-sector domain. The Young modulus and Poisson ratio are $E = 1e+6$ and $\nu = 0.4999$ respectively. The condition number *cond* and PCG iteration counts it. of the FETI-DP preconditioner are reported as a function of the number of subdomains N and mesh size $1/h$, while keeping fixed $p = 2,\ k = 1$ (pressure), $p = 3,\ k = 1$ (displacement) NURBS spaces and $k_\Gamma = 1$. Both ρ-scaling and stiffness scaling are considered. As in the previous test for the Stokes system, the results show that the proposed preconditioner is scalable, since moving along the diagonals of the table the condition number is bounded from above by a constant independent of N. Moving instead along the rows of the table, we verify the bound of Theorem 4.1: with ρ-scaling, the condition numbers seem to grow as $\log^2(H/h)$, while, with stiffness-scaling, the growth in H/h is super-linear.

5.5. AIE system: FETI-DP robustness when $\nu \to 0.5$

We test the behavior of the FETI-DP preconditioner when the material becomes almost incompressible, i.e. when the Poisson ratio ν approaches 0.5. The ring-sector domain is discretized by a mesh of size $h = 1/64$, subdivided into $N = 8 \times 8$ subdomains as in Fig. 1. The NURBS discretization spaces are the generalized Taylor–Hood elements $p = 2,\ k = 1$ for pressures, $p = 3,\ k = 1$ for displacements (top) and $p = 3,\ k = 2$ for pressures, $p = 4,\ k = 2$ for displacements (bottom). The Young modulus is fixed to $E = 6e + 6$. The results reported in Table 6 show clearly that the FETI-DP method, with both ρ-scaling and stiffness-scaling, is robust when $\nu \to 0.5$, since the condition number and PCG iteration counts appear to be bounded by a constant value.

Table 5
AIE system. FETI-DP PCG in ring-sector domain: condition number *cond* and iteration counts it. as a function of the number of subdomains N and mesh size $1/h$ for $p = 2,\ k = 1$ (pressure) and $p = 3,\ k = 1$ (displacement) NURBS, $k_\Gamma = 1$. The elastic parameters are $E = 1e + 6$ and $\nu = 0.4999$.

ρ-scaling										
N	$1/h = 8$		$1/h = 16$		$1/h = 32$		$1/h = 64$		$1/h = 128$	
	cond	it.	*cond*	it.	*cond*	it.	*cond*	it.	*cond*	it.
2×2	14.37	29	10.94	30	19.83	30	23.20	30	27.64	30
4×4			19.22	34	22.99	36	28.90	39	35.55	42
8×8					20.08	38	25.62	40	32.83	43
16×16							21.20	39	26.31	42
32×32									21.28	39
Stiffness-scaling										
2×2	13.98	25	23.17	28	42.73	30	85.97	34	182.36	41
4×4			18.75	34	29.22	40	53.12	52	104.13	63
8×8					20.08	37	31.76	45	58.24	58
16×16							20.39	38	32.89	46
32×32									20.58	37

Table 6
AIE system. FETI-DP PCG in ring-sector domain: condition number *cond*, maximum and minimum eigenvalues λ_{max}, λ_{min}, iteration counts it. as a function of the Poisson ratio ν. for spline spaces $p = 2,\ k = 1$ and $p = 3,\ k = 2$. Fixed fine mesh $1/h = 64$, subdomains mesh $1/H = 8$, Young modulus $E = 6e + 6$.

$p = 2,\ k = 1$ NURBS, $k_\Gamma = 1$								
ν	ρ-scaling				Stiffness-scaling			
	cond	λ_{max}	λ_{min}	it.	*cond*	λ_{max}	λ_{min}	it.
0.35	13.23	7.75	5.86e−1	30	18.16	9.50	5.23e−1	35
0.45	19.97	7.72	3.87e−1	36	25.64	9.19	3.58e−1	41
0.49	24.31	7.71	3.17e−1	39	30.36	9.05	2.98e−1	44
0.499	25.49	7.71	3.02e−1	40	31.63	9.02	2.85e−1	45
0.4999	25.62	7.71	3.01e−1	40	31.76	9.02	2.84e−1	45
0.49999	25.63	7.71	3.01e−1	40	31.77	9.02	2.84e−1	45
0.499999	25.63	7.71	3.01e−1	40	31.77	9.02	2.84e−1	45
0.5	25.63	7.71	3.01e−1	40	31.77	9.02	2.84e−1	45
$p = 3,\ k = 2$ NURBS, $k_\Gamma = 2$								
ν	ρ-scaling				Stiffness-scaling			
	cond	λ_{max}	λ_{min}	it.	*cond*	λ_{max}	λ_{min}	it.
0.35	96.48	52.82	5.74e−1	86	31.75	16.54	5.21e−1	48
0.45	146.39	52.82	3.61e−1	105	45.62	16.13	3.54e−1	57
0.49	178.32	52.82	2.96e−1	115	54.43	15.95	2.93e−1	63
0.499	186.93	52.82	2.83e−1	118	56.82	15.90	2.80e−1	64
0.4999	187.79	52.82	2.81e−1	118	57.06	15.90	2.79e−1	64
0.49999	187.88	52.82	2.81e−1	118	57.09	15.90	2.78e−1	64
0.499999	187.89	52.82	2.81e−1	118	57.09	15.90	2.78e−1	64
0.5	187.89	52.82	2.81e−1	118	57.09	15.90	2.78e−1	64

5.6. AIE system: FETI-DP robustness with respect to jumping coefficients

We finally test the performance of the FETI-DP preconditioner when the elastic coefficients E and ν have discontinuities across the subdomain interfaces. The ring-sector domain is discretized with a mesh size $h = 1/64$ and subdivided into $N = 8 \times 8$ subdomains. The NURBS discretization spaces are the generalized Taylor–Hood elements $p = 2,\ k = 1$ for pressures, $p = 3,\ k = 1$ for displacements (left) and $p = 3,\ k = 2$ for pressures,

Table 7
AIE system. FETI-DP PCG robustness with respect to jump discontinuities in E and ν. Outside the central jump region of 4×4 subdomains $E = 6.e+3$ and $\nu = 0.3$. In the checkerboard test for E, $E = 6e+3$ or $E = 6e+7$ and $\nu = 0.3$, while in the checkerboard test for ν, $E = 6e+3$ and $\nu = 0.3$ or $\nu = 0.4999$. Condition number *cond*, extremal eigenvalues $\lambda_{max}, \lambda_{min}$ and iteration counts it. Fixed $1/h = 64$, $N = 8 \times 8$, $H/h = 8$, $k_\Gamma = 0$.

Jumping coefficient E

	E	$p=2,\ k=1$ NURBS				$p=3,\ k=2$NURBS			
		cond	λ_{max}	λ_{min}	it.	*cond*	λ_{max}	λ_{min}	it.
Central jump	6e+3	20.15	14.13	7.01e−1	36	22.39	15.84	7.08e−1	38
	6e+4	24.43	14.20	5.81e−1	38	27.31	15.96	5.84e−1	40
	6e+5	27.26	14.39	5.28e−1	39	30.46	16.18	5.31e−1	43
	6e+6	27.72	14.41	5.20e−1	40	30.89	16.22	5.25e−1	43
	6e+7	27.74	14.42	5.20e−1	40	30.94	16.22	5.24e−1	43
Checkerboard E		29.33	14.20	4.84e−1	43	32.42	15.92	4.91e−1	46

Jumping coefficient ν

	ν	$p=2,\ k=1$ NURBS				$p=3,\ k=2$NURBS			
		cond	λ_{max}	λ_{min}	it.	*cond*	λ_{max}	λ_{min}	it.
Central jump	0.3	20.15	14.13	7.01e−1	36	22.39	15.84	7.08e−1	38
	0.45	32.44	13.87	4.28e−1	44	36.00	15.51	4.31e−1	46
	0.49	37.08	13.80	3.72e−1	46	41.36	15.43	3.73e−1	50
	0.499	38.28	13.79	3.60e−1	47	42.62	15.41	3.62e−1	50
	0.4999	38.46	13.79	3.58e−1	48	42.75	15.41	3.60e−1	50
	0.49999	38.46	13.79	3.58e−1	48	42.76	15.41	3.60e−1	50
Checkerboard ν		48.08	13.69	2.85e−1	51	53.47	15.29	2.86e−1	53

$p = 4,\ k = 2$ for displacements (right). At the subdomain boundaries we reduce the local regularity to the minimum value $k_\Gamma = 0$, which is sufficient for optimal approximation order in the presence of jumps in the material data. We consider two tests: one with a central jump in a region consisting of the 4×4 central subdomains (see Fig. 1, center), where the material parameters jump from $E = 6.e + 3,\ \nu = 0.3$ outside the central region to the values indicated in Table 7 inside the central region; a second test with a checkerboard distribution (see Fig. 1, right), where E jumps from $E = 6e + 3$ to $E = 6e + 7$ while $\nu = 0.3$ everywhere (top table) or ν jumps from $\nu = 0.3$ to $\nu = 0.4999$ while $E = 6e + 3$ everywhere (bottom table). The results reported in Table 7 show that the FETI-DP preconditioner is very robust for both jumps in E and ν, since all the quantities (condition number, extremal eigenvalues and PCG iterations) do not deteriorate with the jump.

6. Conclusions

We have developed a FETI-DP type domain decomposition preconditioner for isogeometric discretizations of the Stokes and mixed linear elasticity systems. This work extends to isogeometric discretizations the method proposed by Li and Tu in their pioneering papers [13,14] for finite element discretizations of the Stokes system. Following the algebraic theory of [14] and applying some isogeometric technical tools developed in our previous works [5,10], we can prove that the proposed FETI-DP method is scalable in the number of subdomains and quasi-optimal in the ratio of subdomain and element sizes. Numerical experiments in the plane have confirmed the scalability and quasi-optimality of the proposed method.

The numerical tests investigating the behavior of the preconditioner with respect to spline polynomial degree and regularity have shown that, in case of maximal subdomains interface regularity $k_\Gamma = p - 1$, the FETI-DP preconditioner works fine for $p = 2, 3, 4$ and starts degenerating for $p \geq 5$. The reason of such sub-optimal behavior for $p \geq 5$ and maximal interface regularity could be attributed to the non-optimal choice of scaling functions, as observed in our previous isogeometric BDDC paper [5] for scalar elliptic problems. A possible remedy could be the use of deluxe scaling functions, see e.g. [10], but the extension of deluxe scaling to saddle point problems is still an open problem even for standard finite element discretizations. In case of reduced subdomains interface regularity, instead, the FETI-DP preconditioner presents a quasi-optimal behavior up to $p = 8$. Finally, further numerical tests

have shown the robustness of the FETI-DP solver with respect to domain deformations, material incompressibility and the presence of discontinuities of the elastic coefficients across subdomains.

Acknowledgment

The authors were partially supported by grants of INDAM-GNCS 2015-2016.

References

[1] T.J.R. Hughes, J.A. Cottrell, Y. Bazilevs, Isogeometric analysis: CAD, finite elements, NURBS, exact geometry, and mesh refinement, Comput. Methods Appl. Mech. Engrg. 194 (2005) 4135–4195.
[2] J.A. Cottrell, T.J.R. Hughes, Y. Bazilevs, Isogeometric Analysis, in: Towards integration of CAD and FEA, Wiley, 2009.
[3] S.K. Kleiss, C. Pechstein, B. Jüttler, S. Tomar, IETI - isogeometric tearing and interconnecting, Comput. Methods Appl. Mech. Engrg. 247–248 (2012) 201–215.
[4] L. Beirão da Veiga, D. Cho, L.F. Pavarino, S. Scacchi, Overlapping Schwarz methods for isogeometric analysis, SIAM J. Numer. Anal. 50 (3) (2012) 1394–1416.
[5] L. Beirão da Veiga, D. Cho, L.F. Pavarino, S. Scacchi, BDDC preconditioners for isogeometric analysis, Math. Models Methods Appl. Sci. 23 (6) (2013) 1099–1142.
[6] K. Gahalaut, J. Kraus, S. Tomar, Multigrid methods for isogeometric discretization, Comput. Methods Appl. Mech. Engrg. 253 (2013) 413–425.
[7] L. Beirão da Veiga, D. Cho, L.F. Pavarino, S. Scacchi, Isogeometric Schwarz preconditioners for linear elasticity systems, Comput. Methods Appl. Mech. Engrg. 253 (2013) 439–454.
[8] A. Buffa, H. Harbrecht, A. Kunoth, G. Sangalli, BPX-preconditioning for isogeometric analysis, Comp. Meth. Appl. Mech. Engrg. 265 (2013) 63–70.
[9] N. Collier, L. Dalcin, D. Pardo, V.M. Calo, The cost of continuity: Performance of iterative solvers on isogeometric finite elements, SIAM J. Sci. Comput. 35 (2) (2013) A767–A784.
[10] L. Beirão da Veiga, L.F. Pavarino, S. Scacchi, O.B. Widlund, S. Zampini, Isogeometric BDDC preconditioners with deluxe scaling, SIAM J. Sci. Comput. 36 (3) (2014) A1118–A1139.
[11] M. Donatelli, C. Garoni, C. Manni, S. Serra-Capizzano, H. Speleers, Robust and optimal multi-iterative techniques for IgA Galerkin linear systems, Comp. Meth. Appl. Mech. Engrg. 284 (2015) 230–264.
[12] A. Bressan, G. Sangalli, Isogeometric discretizations of the Stokes problem: stability analysis by the macroelement technique, IMA J. Numer. Anal. 33 (2) (2011) 629–651.
[13] J. Li, X. Tu, A nonoverlapping domain decomposition method for incompressible Stokes equations with continuous pressures, SIAM J. Numer. Anal. 51 (2013) 1235–1253.
[14] X. Tu, J. Li, A FETI-DP type domain decomposition algorithm for three-dimensional incompressible Stokes equations, SIAM J. Numer. Anal. 53 (2) (2015) 720–742.
[15] L.F. Pavarino, O.B. Widlund, Iterative substructuring methods for spectral element discretizations of elliptic systems. II. Mixed methods for linear elasticity and Stokes flow, SIAM J. Numer. Anal. 37 (1999) 375–402.
[16] L.F. Pavarino, O.B. Widlund, Balancing Neumann-Neumann methods for incompressible Stokes equations, Comm. Pure Appl. Math. 55 (2002) 302–335.
[17] P. Goldfeld, L.F. Pavarino, O.B. Widlund, Balancing Neumann-Neumann preconditioners for mixed approximations of heterogeneous problems in linear elasticity, Numer. Math. 95 (2003) 283–324.
[18] L. Beirão da Veiga, C. Lovadina, L.F. Pavarino, Positive definite balancing Neumann- Neumann preconditioners for nearly incompressible elasticity, Numer. Math. 104 (2006) 271–296.
[19] A. Toselli, O.B. Widlund, Decomposition Methods: Algorithms and Theory, in: Computational Mathematics, vol. 34, Springer-Verlag, Berlin, 2004.
[20] C.R. Dohrmann, A Substructuring Preconditioner for Nearly Incompressible Elasticity Problems. Tech. Rep. SAND2004-5393, Sandia National Laboratories, Albuquerque, 2004.
[21] J. Li, A dual-primal FETI method for incompressible Stokes equations, Numer. Math. 102 (2005) 257–275.
[22] J. Li, O.B. Widlund, BDDC algorithms for incompressible Stokes equations, SIAM J. Numer. Anal. 44 (2006) 2432–2455.
[23] L.F. Pavarino, O.B. Widlund, S. Zampini, BDDC preconditioners for spectral element discretizations of almost incompressible elasticity in three dimensions, SIAM J. Sci. Comput. 32 (2010) 3604–3626.
[24] S. Zampini, X. Tu, Adaptive multilevel BDDC deluxe algorithms for flow in porous media, (2016) submitted for publication.
[25] P. Goldfeld, Balancing Neumann-Neumann Preconditioners for the Mixed Formulation of Almost-Incompressible Linear Elasticity. Tech. Rep. TR2003-847, Courant Institute of Mathematical Sciences, New York University, New York, 2003.
[26] C.R. Dohrmann, O.B. Widlund, An overlapping Schwarz algorithm for almost incompressible elasticity, SIAM J. Numer. Anal. 47 (2009) 2897–2923.
[27] C.R. Dohrmann, O.B. Widlund, A hybrid domain decomposition method for compressible and almost incompressible elasticity, Internat. J. Numer. Methods Engrg. 82 (2010) 157–183.
[28] A. Klawonn, L.F. Pavarino, Overlapping Schwarz methods for mixed linear elasticity and Stokes problems, Comput. Methods Appl. Mech. Engrg. 165 (1998) 233–245.
[29] A. Klawonn, L.F. Pavarino, A comparison of overlapping Schwarz methods and block preconditioners for saddle point problems, Numer. Linear Algebra Appl. 7 (2000) 1–25.

[30] F.N. Hwang, X.-C. Cai, A parallel nonlinear additive Schwarz preconditioned inexact Newton algorithm for incompressible Navier–Stokes equations, J. Comput. Phys. 204 (2005) 666–691.
[31] F.N. Hwang, X.-C. Cai, A class of parallel two-level nonlinear Schwarz preconditioned inexact Newton algorithms, Comput. Methods Appl. Mech. Engrg. 196 (2007) 1603–1611.
[32] A.T. Barker, X.-C. Cai, Two-level Newton and hybrid Schwarz preconditioners for fluid–structure interaction, SIAM J. Sci. Comput. 32 (2010) 2395–2417.
[33] P.F. Fischer, An overlapping Schwarz method for spectral element solution of the incompressible Navier–Stokes equations, J. Comput. Phys. 133 (1997) 84–10.
[34] M. Cai, L.F. Pavarino, O.B. Widlund, Overlapping Schwarz methods with a standard coarse space for almost incompressible linear elasticity, SIAM J. Sci. Comput. 37 (2) (2015) A811–A830.
[35] D. Boffi, F. Brezzi, M. Fortin, Mixed Finite Element Methods and Applications, in: Computational Mathematics, vol. 44, Springer-Verlag, Berlin, 2013.
[36] L.L. Schumaker, Spline Functions: Basic Theory, third ed, Cambridge Mathematical Library, Cambridge University Press, Cambridge, 2007.
[37] Y. Bazilevs, L. Beirão da Veiga, J.A. Cottrell, T.J.R. Hughes, G. Sangalli, Isogeometric analysis: approximation, stability and error estimates for h-refined meshes, Math. Models Methods Appl. Sci. 16 (2006) 1–60.
[38] C. De Falco, A. Reali, R. Vazquez, GeoPDEs: a research tool for isogeometric analysis of PDEs, Adv. Engrg. Softw. 42 (12) (2011) 1020–1034.